Periodic Density Functional Theory Studies of Vanadia−Titania Catalysts: Structure and Stability of the Oxidized Monolayer

Andrea Vittadini*

CNR Institute of Molecular Science and Technologies (CNR-ISTM), Consortium for Science and Technology of Materials (INSTM), Chemistry Department, University of Padova, via Marzolo 1, I-35131 Padova, Italy

Annabella Selloni

Chemistry Department, Princeton University, Princeton, New Jersey 08540

Received: December 15, 2003; In Final Form: March 12, 2004

We present first-principles calculations of vanadia−titania catalysts at V-coverages up to one monolayer. Realistic slab models are built where vanadate species (VO_x) are grafted onto hydroxyls existing at the (001) surfaces exposed by the TiO_2-anatase support. The structure and stability of several microscopic models of oxidized VO_x (sub)monolayers have been computed. We find that tetrahedrally coordinated monovanadate units are stable for low V-coverages, but are readily converted to divanadate units for higher coverages. The structure of these units is closely related to that of a recently proposed model of the (1×4) reconstruction of the dehydroxylated (001) anatase surface, where arrays of surface bridging oxygens are replaced by tetrahedral structures. High V-coverages (>0.5 ML) can be obtained if the substrate acquires the structure of a bulk-terminated TiO_2(001) surface. In this case, a stable polymeric structure can be formed, which is structurally related to a (100)-oriented vanadia layer. At the same time, the coordination around the V atoms changes from four to five, in agreement with experiment. Thick vanadia layers are found to be unstable with respect to decomposition into separate supported-monolayer and bulk vanadia phases.

1. Introduction

Titania-supported vanadium oxide catalysts are widely used for several industrial processes, such as *o*-xylene oxidation to phthalic anhydride,[1] methanol oxidation,[2] and the selective catalytic reduction of NO ($DeNO_x$ process).[3] These industrial catalysts are usually prepared by impregnation with a vanadium salt (e.g., ammonium metavanadate, NH_4VO_3), followed by a calcination treatment. In the resulting materials, many vanadia phases are present,[1] thus making the origin of the catalytic properties of the system difficult to be traced back. More direct information can be obtained from "cleaner" systems, which can be prepared by several approaches. Among them, particularly interesting are grafting techniques, where molecular precursors such as $VOCl_3$ or $VO(OR)_3$ are attached to the surface by means of reactions like the following:

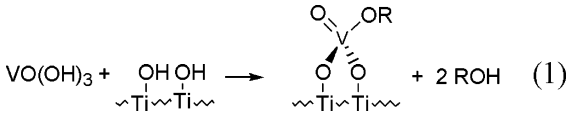

Grafting allows a more careful control of the growth of vanadia species (VO_x).[4] In this way, the so-called vanadia−titania (VO_x/TiO_2) "monolayer catalysts" can be obtained, where the term "monolayer" is used to indicate a number density of V atoms equal to that of surface Ti atoms, with the assumption that the titania surface is completely covered by $VO_{2.5}$ stoichiometric units.[1] However, it has been found that a large fraction of the support surface is *not* covered by vanadia, even for loadings higher than the theoretical monolayer coverage.[5] It has also been reported that "true" monolayer species (also called "insoluble") actually amount to ∼20−30% of a theoretical monolayer.[1,6] This suggests that only a small portion of titania is suitable to support *stable* vanadia layers.

Concerning the catalyst's structure, early studies suggested the formation of ordered layers of vanadia grown on the (001) surface of TiO_2-anatase.[7,8] By contrast, X-ray absorption fine structure spectroscopy (XAFS) measurements found that the active phase is amorphous in nature.[9] Subsequent studies carried out on monolayer catalysts shed light on this issue,[4] showing that successive grafting processes can be carried out. This was interpreted as an indication that deposited species take the form of tetrahedral hydroxo-vanadyl moieties ═VO(OH) (where the "═" symbol is used to represent the two bonds which anchor V to substrate O atoms). Such species can in turn either react with new incoming precursor molecules, or undergo condensation processes yielding polyvanadate species. Structural ^{51}V−NMR[10,11] and XAFS[9] measurements indicate that V atoms are initially in a tetrahedral environment, and turn to higher coordination numbers by increasing the coverage. When the V-loading is further increased, an amorphous vanadia layer is formed, and, subsequently, vanadia crystals start to appear.[1]

Recently, several computational studies of vanadia−titania catalysts have been reported.[12−17] Irrespective of the differences in computational and modeling approaches, these studies can be divided on the basis of the chemical criteria followed to model the layer. In one group of investigations[12] the active layer is assumed to be a weakly perturbed V_2O_5 layer, and the model essentially consists of a vanadia(001) surface.[18] Clearly, this picture is better suited to describe supramonolayer vanadia

* Corresponding author. Fax: +39-049-8275161. E-mail: andrea.vittadini@unipd.it.

10.1021/jp037869z CCC: $27.50
Published on Web 05/04/2004

species, i.e., those species not directly attached to the support, which are present at very high V-loadings. In other studies,[13−15,17] attention is focused on the vanadia/titania interface, by considering V-species possibly present *at* or *on* the anatase surfaces. However, the supporting surface is typically assumed to be the dehydroxylated, unreconstructed (001) anatase surface, whereas it is known that anatase(001) is actually either hydroxylated, or, after thermal treatments, (1 × 4)-reconstructed.[19−23] The presence of OH groups on the support surface has been taken into consideration by Khaliullin and Bell,[16] who modeled the active species by taking a tetrahedral VO_4 unit linked to three OH-saturated Ti atoms, and fixing the Ti−Ti and Ti−V distances at the values indicated by XAFS measurements. Also Ferreira and Volpe[13] built cluster models of the hydroxylated TiO_2(001) surface by simply placing H atoms on top of the bridging oxygen anions. From the above short summary, it seems fair to conclude that in most theoretical investigations so far appeared two important aspects of the system, i.e., the structure of the support and the role of support hydroxyls have been either ignored or treated with rather crude models. Extended models of the V_2O_5/TiO_2 interface have been studied by Sayle et al.[17] by means of simulations based on force fields. However, as pointed out by the same authors, the reliability of their calculated interfacial energies as a mean to assess the stability of these systems is unclear.

In this work, we investigate the structure of submonolayer and monolayer vanadia−titania catalysts by using first-principles computational techniques with large slab models that we construct on the basis of our previous studies of anatase surfaces.[19,20,24,25] Models of the catalyst are built through a "bottom-up" strategy which mimics the experimental grafting process: increasingly complex vanadia structures are grown via the condensation reaction of a model vanadate precursor, $VO(OH)_3$, with the surface OH groups, starting from those natively present on the anatase(001) surface. The present study is limited to fully oxidized VO_x structures. Formation of reduced layers will be addressed in a forthcoming paper.

2. Theoretical Approach and Computational Setup

Structural optimization were performed in the Car-Parrinello scheme,[26] using a combined electronic and ionic damped dynamics algorithm, in conjuction with a preconditioning scheme.[27] The so-called PBE functional was used within the generalized gradient approximation (GGA)[28] to describe exchange and correlation effects.

"Ultra-soft" relativistic pseudopotentials[29] were used for all the ions. To increase the accuracy of the results, we made use of small cores, including the 1s state for O, and the 1s, 2s, and 2p states for Ti and V. The smooth part of the wave functions was expanded in plane waves with a kinetic energy cutoff of 25 Ry, while the cutoff for the augmented electron density was 200 Ry. The theoretical[20] anatase lattice constants were used. The support, i.e., the anatase(001) surface, and the catalyst were modeled by using a periodically repeated slab of four Ti layers, similar to that employed in ref 19. In most calculations, a (2 × 2) supercell was adopted (see Figure 1a), but in some cases we also used a larger (3 × 2) supercell, shown in Figure 1b. Atomic relaxations were carried out until residual forces were less than 0.05 eV/Å. VO_x species were introduced only on the upper part of the slab. The lowest two atomic layers of the slab were kept fixed in their bulk positions throughout the calculations. The k-sampling was restricted to the Γ point, as this was found to be adequate in our previous study on the interaction between anatase and water.[19]

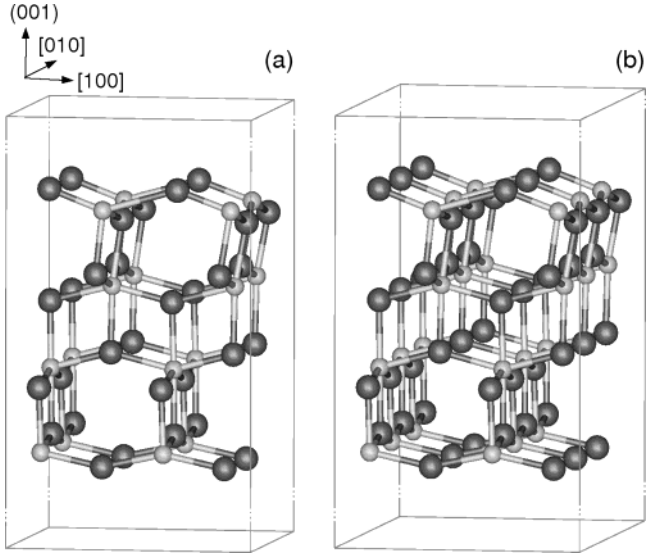

Figure 1. Periodically repeated slabs used in the calculations: (a) (2 × 2) supercell; (b) (3 × 2) supercell. The dimensions are (7.56 × 7.56 × 21.00) Å^3 and (7.56 × 11.36 × 21.00) Å^3, respectively. Pictures of the cells have been truncated along the [001] direction to save space. Structures shown are the clean, unreconstructed. and relaxed anatase-(001) surface. Small balls are Ti atoms, larger balls are oxygen atoms.

For the purpose of obtaining a reference state needed to evaluate the stability of our vanadia−titania interface models, we also performed calculations on the vanadia bulk phase with the PWSCF package.[30] The optimized lattice parameters that we obtain (a = 11.61 Å, b = 3.56 Å, c = 4.68 Å) are in very good agreement both with experiment[31] and with recent Perdew-Wang DFT calculations.[32] As a further check, we computed the stability of several V_xO_y free clusters, and obtained satisfactory agreement with recent results by Vyboishchikov and Sauer.[33]

Results and Discussion

3.1. The Structure of the TiO_2 Support. Anatase supports used for VO_x/TiO_2 catalysts are in a powder/nanocrystalline form. While in principle a large number of different crystallographic surfaces could be exposed, it is well established that the (101) surface is by far the most stable one. In particular, the calculated equilibrium shape for *dehydroxylated* anatase crystals is a truncated square bipyramid where (101) planes form the majority of the total exposed surface,[20] while the remaining (minority) part consists of (001) surfaces. Remarkably, such a shape is observed in both natural crystals and nanocrystals synthesized by various techniques.

Experimental[21,22] and theoretical results[19] indicate that, of the two prevalently exposed (101) and (001) surfaces, only the latter one is able to dissociatively adsorb water. The (101) surface can dissociate water only at oxygen vacancy sites, producing bridging hydroxyls,[34,35] but the density of such defect sites has been found to be quite low.[36] Thus, vanadium molecular precursors can be expected to be prevalently grafted onto the (001) planes exposed by anatase nanocrystals of the support. This is in line with the fact that, even for very high loadings, only a small part of the titania surface is covered by vanadia.[5]

The unreconstructed (001) surface is characterized by chains of 5-fold Ti ions and 2-fold coordinated O ions (the so-called *bridging* oxygens) running along the [100] direction and forming *rows* oriented along the [010] direction (see Figure 1). Under UHV conditions, however, this surface undergoes a (1 × 4) reconstruction,[23] that has been theoretically explained[24] in terms

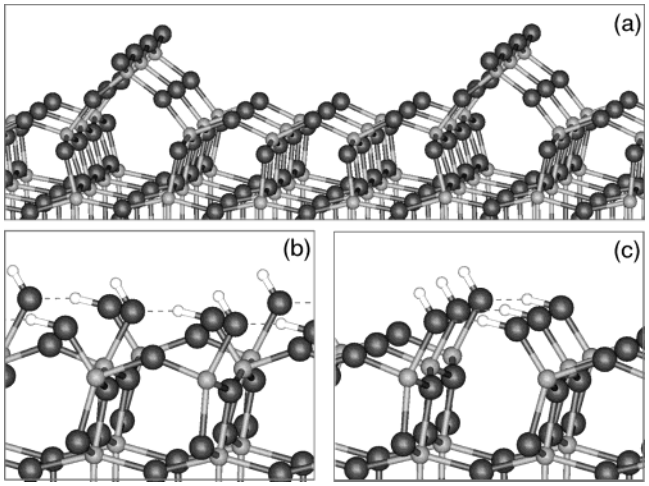

Figure 2. (a) ADM model of the (1 × 4) reconstruction of the clean anatase(001) surface.[24] (b) and (c) Relaxed geometries for two models of the hydroxylated anatase(001) surface with a half-monolayer coverage of dissociatively adsorbed water molecules.[19] Structures refer to the (2 × 2) slab, in the cases where (b) water molecules are adsorbed on sites placed along *different* ⟨010⟩ rows, and (c) water molecules are adsorbed on sites belonging to the *same* ⟨010⟩ row. This gives rise to (2 × 2) ("scrambled") and (2 × 1) ("ordered") superstructures in the two cases, respectively. Note the arrangement of OH groups in hydrogen-bonded *pairs*, and the similarity of the structure changes induced on the surface by hydroxylation with those induced by reconstruction. Ti and O atoms as in Figure 1, H atoms are represented by small white balls. Axes are oriented as in Figure 1.

of the so-called "ad-molecule" (ADM) model, where 1/4 of the bridging oxygen rows are replaced by a $(TiO_3)_n$ "polymer", which has *tetrahedrally* coordinated Ti ions (see Figure 2a). Incidentally, the opening of the oxygen bridges in the ADM model reminds us of that occurring in the case of water adsorption,[19] where half of the bridging oxygens are replaced by pairs of hydrogen-bonded hydroxyls. This similarity suggests that the dissociative adsorption of water on the (001) surface may be driven by the same mechanism of surface stress relief that determines the clean surface reconstruction.[24]

Two different configurations of the hydroxylated (001) surface are shown in Figures 2b and 2c: these corresponds to water adsorption occurring by breaking O-bridges within the *same* or in *different* ⟨010⟩ rows of a (2 × 2) supercell, leading to an "ordered" and "scrambled" superstructure, respectively. We found that the adsorption energy is 1.20 eV per water molecule in the former case, and 1.23 eV in the latter. Such a small difference is not significant: on a thermodynamic basis, hydroxyls can be thus expected to be arranged in a random fashion on the surface.

3.2. Modeling of VO_x Species. Evaluating the relative stability of different VO_x species is not straightforward, because the equilibria governing the formation of the vanadia−titania interface are rather complex, depending on the degree of hydroxylation of the surface, on the presence of water, and on the nature of the vanadium precursor. Furthermore, we should take into account that vanadate species tend to form polymers, which increase in complexity on raising the pH (see, e.g., ref 38). Since catalysts are calcined before use, and layers must be stable against decomposition into separate titania and vanadia phases, we shall refer our calculated formation energies to the bulk phase of V_2O_5 and to the ADM model of the (1 × 4)-reconstructed anatase(001) surface. The energy of the latter is estimated by adding the reconstruction energy, as computed in ref 23, to the energy of a (1 × 1)-unreconstructed (2 × 2) slab. Thus the

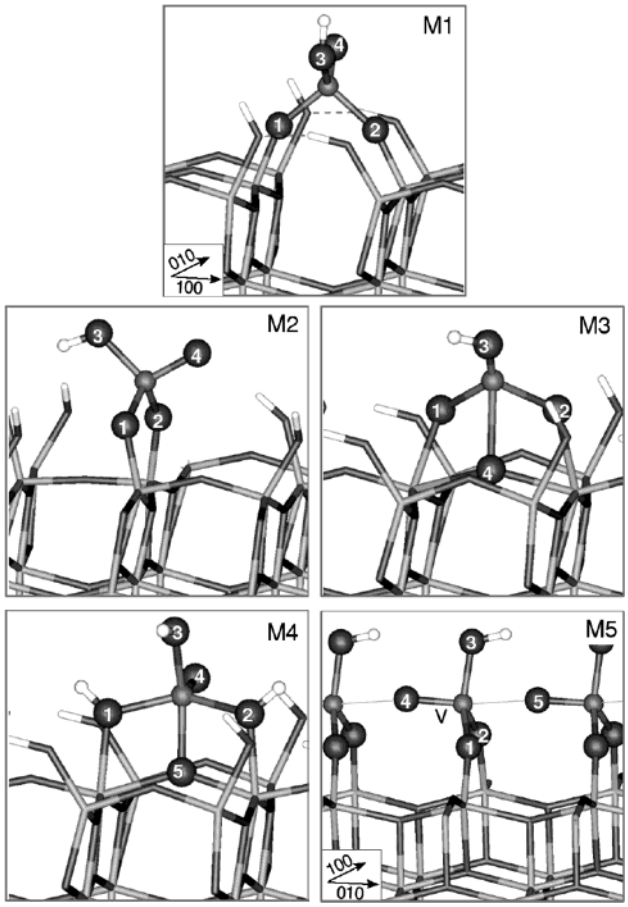

Figure 3. Relaxed structures for model monomeric vanadate units. Atoms belonging to the vanadate unit are depicted in a ball-and-stick representation, whereas all the other ones are shown as "licorice". Notice that the viewpoint for **M5** is rotated by 90° with respect to the other structures.

formation process of the VO_x layer will be described as

$$TiO_2(001)\text{-}(1\times 4) + nVO_{2.5}(s) + (m/2)H_2O(l) \xrightarrow{\Delta E^f} TiO_2(001)\text{-}V_nO_xH_m \quad (2)$$

where $x = (5n + m)/2$, and $H_2O(l)$ is a water molecule in the liquid phase, whose energy we evaluate as the sum of the total energy of an isolated water molecule at $T = 0$ K and of the experimental latent heat of vaporization at 298 K.[39]

3.2.1. Monomeric Species. At low V-coverages, relevant species are monomeric hydroxo-vanadyl ═VO(OH) units, ideally obtained via the reaction of a model $VO(OH)_3$ precursor molecule with two adjacent OH groups of the hydroxylated anatase(001) surface, viz.:

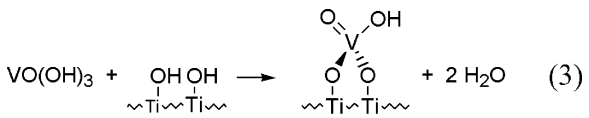

M

Several conformations of these species are possible, depending on the local arrangement of OH groups and on the orientation of the new O−V−O bridges formed on the surface. If grafting occurs by condensing $VO(OH)_3$ with two hydroxyls belonging to the *same* pair, then the V═O and the V−OH bonds will be lying in the same (100) plane (see configuration **M1** of Figure 3). On the other hand, if the condensation occurs with

TABLE 1: Bond Distances (Å and formation energies (eV/(1 × 1), see eq 2) of the Monomeric Vanadate Units Shown in Figure 3. Calculations Were Performed on (2 × 2) Slabs

	M1	M2	M3	M4	M5
ΔE^f	−0.07	+0.26	+0.12	−0.04	+0.03
d(V−O1)	1.75	1.80	1.68	1.92	1.75
d(V−O2)	1.77	1.78	1.70	1.92	1.78
d(V−O3)	1.79	1.79	1.80	1.81	1.82
d(V−O4)	1.60	1.61	1.77	1.60	1.63
d(V−O5)				1.93	2.18
d(O3−H)	0.99	0.99	0.99	0.99	0.99
d(O1−Ti)	1.83	1.85	2.15	2.11	1.83
d(O2−Ti′)	1.80	1.87	2.29	2.14	1.80
d(O4−Ti)			2.27		
d(O4−Ti′)			2.05		

TABLE 2: Selected Bond Distances (Å) and Formation Energies (eV/(1 × 1)) of the divanadate models in Figure 4. Calculations Were Done Using (2 × 2) Slabs

	D1	D2	D3	D4	D5
ΔE^f	−0.08	+0.20	+0.14	−0.01	−0.06
d(V−O1)	1.76	1.79	1.72	2.12	1.72
d(V−O2)	1.78	1.80	1.66	2.05	1.77
d(V−O3)	1.78	1.78	1.80	1.77	1.80
d(V−O4)	1.58	1.59	1.74	1.60	1.60
d(V−O5)				1.94	
d(O1−Ti)	1.83	1.80	2.36	2.12	
d(O2−Ti)	1.80	1.79	2.02	2.05	1.77

hydroxyls of *different* pairs, the bonds will be lying in a (010) plane (see configuration **M2**, Figure 3). Another possible arrangement is **M3**, where the vanadylic oxygen is rotated toward the surface, thus restoring the bridging oxygen of the clean, unreconstructed surface (this could also have been seen as the product of an adduct between the dehydroxylized surface and a hypothetical VO_2OH cluster). Still another possibility is the **M4** structure, which can in turn be viewed either as the result of the addition of a water molecule to **M3**, or as an adduct formed between a $VO(OH)_3$ precursor and a Ti−O−Ti dehydroxylated bridge of the surface.

Relevant geometry parameters for the **M1**−**M5** structures are reported in Table 1. These are in fair agreement with most recent estimates obtained by XAFS spectroscopy,[37] which show that the length of V═O bonds of supported vanadium species is around 1.6 Å, while the V−O ones have a length of about 1.8 Å. Our results are also in agreement with the predictions by Khaliullin and Bell,[16] (1.77 and 1.60 Å for V−O and V═O bond lengths, respectively), although they adopted a rather different model. This indicates that the bond lengths of VO_x species are rather insensitive to the structure of the environment. On one hand, this explains why rather similar geometry parameters are measured for VO_x species grafted onto different substrates. On the other hand, this means that agreement with structural data is not enough to establish the validity of a model.

Formation energies for the above species, reported in Table 1, show that the **M1** structure is quite favorable,[40] whereas **M2** is unstable. This indicates that there is a preferred orientation for tetrahedrally coordinated ═VO(OH), which corresponds to grafting the precursor to OH units belonging to the same pair. The formation energy of **M3** is also high, likely because of the stress introduced by the two rather short V−O1 and V−O2 bonds. The **M4** structure, where these two bonds are considerably longer, is indeed much more stable.

Monolayers with coverage up to $\Theta = 0.5$ ML can in principle be obtained by reacting all the surface hydroxyls with vanadate precursors to form monomeric surface species. In the case of a scrambled OH arrangement (see Figure 2), the formation energy of monomers is practically unchanged with respect to the **M1** low-coverage case. In the case of an ordered OH arrangement, instead, a polymer-like structure (see **M5**, in Figure 3) is formed. However, the formation energy of this structure is *positive* (see Table 1), i.e., ⟨010⟩ arrays of monomers are not stable.

TABLE 3: Formation Energies (eV/1 × 1) and Bond Distances (Å) of VO_x Layers for $\Theta = 1.0$ Coverage. Structures Are Shown in Figure 6. Results Refer to a (2 × 2) Slab

	ML-OH	ML
ΔE^f	−0.01	−0.08
d(V−O1)	2.12	2.04
d(V−O2)	1.79	1.85
d(V−O3)	1.81	1.58
d(V−O4)	1.62	1.77
d(V−O5)	2.20	
d(V−Ob)	2.03	2.03
d(O3−H)	0.99	
d(O1−Ti)	2.06	2.00
d(O2−Ti′)	2.07	2.00
d(O_b-Ti)	2.03	2.01
d(O_b-Ti′)	1.91	1.90

3.2.2. Dimeric Species. As described by Bond,[4] upon increasing the vanadia loading, isolated VO_x units tend to form different species, which are generically indicated as polyvanadates (see, e.g., ref 1). We first studied the formation of the simplest possible polyvanadate, i.e., a divanadate. This can be formally obtained by dimerizing two ═VO(OH) units, which yields a ═VO−O−VO═ divanadate species:

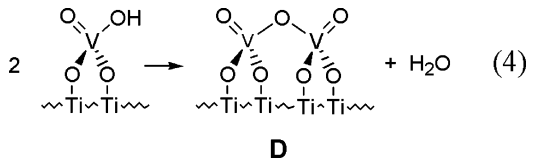

(4)

D

Formation energies reported in Table 2 show that dimeric units prefer to be oriented on the surface similarly to what was found for monomeric species: configuration **D1** is considerably more stable with respect to the **D2** "rotated" one. There is a remarkable structural similarity between **D1** and the ADM model of the clean (001)-1 × 4 reconstructed surface (see Figure 2a and **D1**). In both cases, there are sequences of tetrahedrally coordinated metal atoms running in the [010] direction. As the (1 × 4) reconstruction strongly stabilizes the clean (001) anatase surface, **D1** is also very stable.

We also studied the structure and stability of a recently proposed[15] "flat" dimer (**D3**), which is obtained by placing a V_2O_5 cluster on top of the unreconstructed anatase(001) surface. We find that also the **D3** dimer is largely unfavored with respect to the "tetrahedral" **D1** dimer. To check the influence of possible repulsive interactions between consecutive images of the dimer units (all the calculations so far described were performed on a (2 × 2) supercell), we performed further calculations for **D1** and **D3** in a (3 × 2) supercell, by considering both a final configuration where the non-reacted support OH groups remain on the surface, and one where the non-reacted OH groups are eliminated. We found that the stability of the dimers is increased when the spacing between the units is larger, indicating that a sizable repulsion between adjacent dimeric units is indeed present. However, the tetrahedral dimer remains ∼0.2 eV/1 × 1 more stable than the flat one.

Other stable dimeric structures are **D4** and **D5**. **D4** can be viewed as the dimer of **M4** or as the product of the (favorable) dissociative adsorption of two water molecules on **D3**. This species carries V═O groups, as suggested by experiments, and it is more stable than **D3**, but is it still unfavored by 0.08 eV

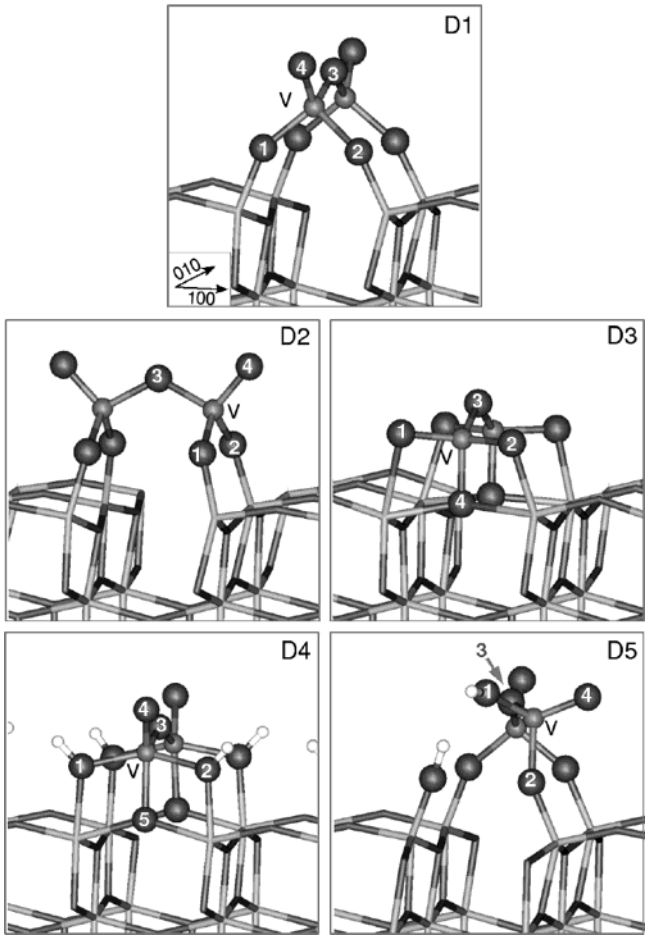

Figure 4. Relaxed structures of dimeric vanadate units grafted onto the hydroxylated anatase(001) surface. Atoms are represented as in Figure 3.

with respect to **D1**. Though low, this energy difference is significant, because the **D4** → **D1** + H_2O process is favored by increasing the temperature, as during calcination. In the **D5** structure, one Ti−O−V bond is hydrolyzed so that this V atom is anchored to the surface by a single bond. This structure is stabilized through formation of a hydrogen bond between the V−OH and the V═O groups of adjacent units. However, similarly to **D4**, this structure should also be readily converted to **D1** by calcination.

3.2.3. Trimers and Polymeric Species. By adding a monomer to a dimer, viz., a trimer species can be formed. Electron

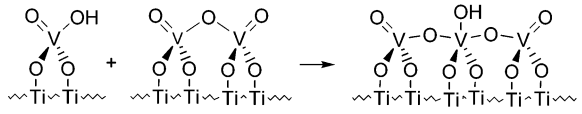

(5)

T1

counting suggests a 5-fold coordination for the central V atom, which can be obtained only if it carries a OH group. The equilibrium structure of such a trimer (**T1**) is reported in Figure 5: the central V atoms assumes a trigonal bipyramidal (TBP) configuration, whereas the geometrical parameters of the tetrahedral terminal V atoms are almost identical to those obtained in the case of the dimeric unit.

The stability of **T1** is found to be lower with respect to isolated monomers and dimers, but considerably higher with respect to a periodic system built by alternating monomers and dimers along [010]. This suggests that, although not particularly

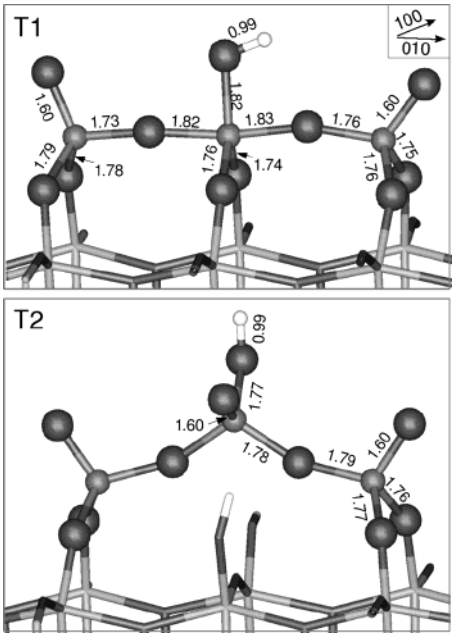

Figure 5. Equilibrium structures for a trimeric unit. Distances are in Å. ΔE^f are +0.03 (**T1**) and −0.05 (**T2**) eV/(1 × 1). These structures were calculated using a 3 × 2 slab.

stable, trimer species could be present in situations where a perfect pairing of monomers cannot be obtained during calcination.

A different kind of trimeric species can be formed on a surface with scrambled hydroxyls. This can be formally obtained by condensing a $VO(OH)_3$ precursor with two monomeric units, namely: For this trimer we find a formation energy of −0.05

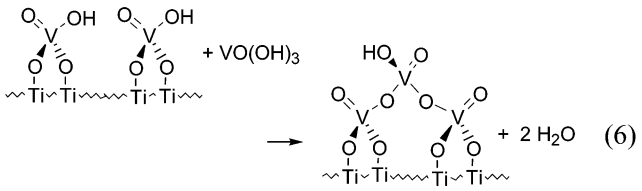

(6)

T2

eV/1 × 1, which is the lowest among all examined trimer models.

We previously mentioned that polymeric VO_x species are present at the surface of the catalyst for high V-loadings. Since our most stable models for the monovanadate and divanadate species are similar in structure to the chains which are present in the ADM model of the $TiO_2(001)-(1 \times 4)$ surface, we tried to construct polymeric VO_x species similar to the polymeric chains of the ADM model. However, none of our models turned out to be stable.

3.2.4. Epitaxial Layers. Several experiments provide evidence that, at high V-loading, full vanadia monolayers are present. Since there is no way in which full monolayers can be modeled in terms of the species that we have so far investigated, we decided to examine coherent vanadia/titania interfaces of the type previously studied by Sayle et al.[17] These authors computed the formation energies of the (001)/(001), the (200)/(001), and the (011)/(001) V_2O_5/TiO_2 interfaces by simulations based on force fields, and predicted a stability sequence (011)/(001) > (001)/(001) > (200)/(001). However, they also found that a good charge matching could be obtained at the $V_2O_5(200)/TiO_2(001)$ interface, thanks to a substantial vertical relaxation of the

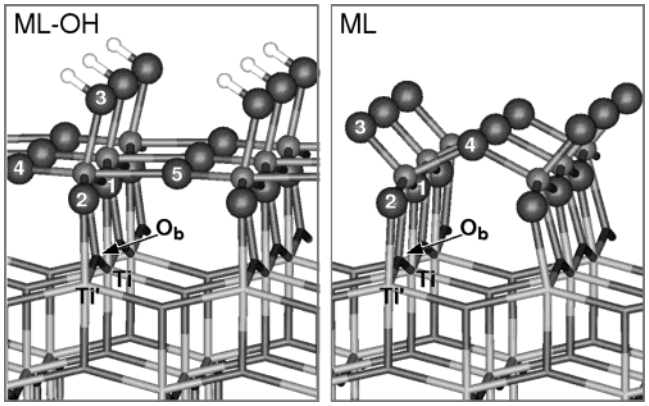

Figure 6. Equilibrium structures for $\Theta = 1.0$ coverage. Axes as in Figure 5.

overlayer. This destabilizes thick overlayers but it is less relevant when a single monolayer is present, which is the case of interest in this work. We have thus taken the $V_2O_5(100)/TiO_2(001)$ interface as a model of the vanadia/titania monolayer structure.

It may be helpful to think of this interface as the result of a sort of surface polymerization process involving **M4** monomers. In such a process, all the lateral OH groups are eliminated by condensation, while the top OH group is either eliminated (to allow the layer to increase in thickness), or maintained (if we are dealing with the topmost monolayer). The final product of this process for a 1-ML coverage (**ML-OH**) is shown in Figure 6. The equilibrium structure is in qualitative agreement with that obtained by Sayle et al.[17] for a 3-ML coverage. However, because in our case the vanadia is only one layer thick, we find that the interface is stable with respect to the decomposition into titania and vanadia separate phases. Clearly, this is not likely to be the case if we increase the coverage because the vanadia layer is strongly distorted with respect to the bulk structure. Indeed, for a hydroxylated 2ML-thick $V_2O_5(100)/TiO_2(001)$ interface we find a very high formation energy, 0.54 eV/1 $\times$ 1, implying that thick vanadia layers should readily decompose into a supported monolayer and bulk vanadia separate phases. It is remarkable that the optimized structure of the titania surface is practically identical to that of the bulk (see the Ob-Ti bond distances), suggesting that the (100)-oriented vanadia monolayer is able to terminate very efficiently the titania surface.

By eliminating the residual OH groups, the dehydroxylated interface **ML** shown in Figure 6 is obtained. This structure bears some resemblance to that of the **D1** dimers, but it actually corresponds to a polymeric structure. The stability of **ML** is very high, and it is practically identical to that of **D1**, which is the most stable structure we have found for $\Theta = 0.5$. Furthermore, the local coordination around V is quite similar to that inferred by very recent XANES calculations:[41] the only difference is that in our model a bridging oxygen replaces a vanadylic one.

Conclusion

In conclusion, we have used state-of-the-art DFT calculations in order to study fully oxidized monolayer vanadia−titania catalysts. The structure and the stability of several models have been computed by considering the condensation of model $VO(OH)_3$ precursors with the OH groups present on the (001) anatase surface. We have determined which VO_x species are thermodynamically stable, depending on the V-coverage. Our results confirm and explain several experimental findings. In particular we find the following: (*i*) for low coverages ($\Theta < 0.5$), species containing tetrahedrally coordinated VO_x are formed; (*ii*) these can contain hydroxo-vanadyl, ═VO(OH), and divanadate, ═V(O)−O−V(O)═, moieties: the former are stable only when they are isolated; (*iii*) tetrahedral VO_x species modify the support (001) surface in a way similar to the (1 $\times$ 4) reconstruction of the clean surface, which explains their stability; (*iv*) when a full VO_x monolayer is present, the structural modifications of the support surface are rather small, i.e., the VO_x layer seems capable of restoring an optimal surface termination; (*v*) at the same time, the coordination number of V atoms changes from four to five; (*vi*) the structure of the monolayer can be related to that of a (100)-oriented vanadia film; (*vii*) multilayer films are unstable with respect to decomposition into separate supported-monolayer and bulk vanadia phases; (*viii*) overall, bond distances found in the proposed models are compatible with most accurate experimental determinations.

As mentioned in the Introduction, the structure of the monolayer is usually interpreted with two different models. In one of them,[7] the occurrence of a coherent TiO_2/V_2O_5 interface is predicted. In the other one,[4] the reaction of vanadia molecular precursors with OH groups present on the substrate (grafting) is emphasized. Our results suggest that these models are not mutually exclusive: the grafting model seems to be best suited to describe a situation of low coverage, while the coherent interface model seems more appropriate at high coverage. Even though real surfaces are much more complicated than our models, e.g., because of defects (such as low coordinated ions) which can also play a role on VO_x adsorption, our results should provide a significant contribution to the understanding of the chemistry of vanadia−titania systems, particularly of the effects of changing the vanadia content.

Acknowledgment. The calculations of this work have been performed at the Keck Materials Science Computing Center of the Princeton Materials Institute. The figures of structures were obtained with gOpenMol 2.2.[42]

References and Notes

(1) Grzybowska-Świerkosz, B. *Appl. Catal., A, Gen.* **1997**, *157*, 263.
(2) Forzatti, P.; Tronconi, E.; Elmi, A. S.; Busca, G. *Appl. Catal. A. Gen.* **1997**, *157*, 387.
(3) Busca, G.; Lietti, L.; Ramis, G.; Berti, F. *Appl. Catal., B., Environ.* **1998**, *18*, 1.
(4) Bond, G. C. *Appl. Catal., A., Gen.* **1997**, *157*, 91.
(5) Bond, G. C.; Perez Zurita, J.; Flamerz, S.; Gellings, P. J.; Bosch, H.; Van Ommen, J. G.; Kip, B. J. *Appl. Catal.* **1986**, *22*, 361; Bond, G. C.; Perez Zurita, J.; Flamerz, S. *Appl. Catal.* **1986**, *27*, 353.
(6) Centi, G.; Giamello, E.; Pinelli, D.; Trifirò, F. *J. Catal.* **1991**, *130*, 220. Centi, G.; Pinelli, D.; Trifirò, F.; Ghoussoub, D.; Guelton, M.; Gengembre, L. *J. Catal.* **1991**, *130*, 238.
(7) Vejux, A.; Courtine, P. *J. Solid State Chem.* **1978**, *23*, 93.
(8) Inomata, M.; Mori, K.; Miyamoto, A.; Vi, T.; Murakami, Y. *J. Phys. Chem.* **1983**, *87*, 754.
(9) Kozlowski, R.; Pettifer, R. F.; Thomas, J. M. *J. Phys. Chem.* **1983**, *87*, 5176.
(10) Eckert, H.; Wachs, I. E. *J. Phys. Chem.* **1989**, *93*, 6796.
(11) Lapina, O. B.; Shubin, A. A.; Khabibulin, D. F.; Tershkikh, V. V.; Bodart, P. R.; Amoureux, J.-P. *Catal. Today* **2003**, *2816*, 1.
(12) Topsøe, N. Y.; Dumesic, J. A.; Anstrom, M. *Catal. Lett.* **2001**, *76*, 11. Anstrom, M.; Dumesic, J. A.; Topsøe, N. Y. *Catal. Lett.* **2002**, *78*, 281.
(13) Ferreira, M. L.; Volpe, M. *J. Mol. Catal. A: Chem.* **2000**, *164*, 281.
(14) Kachurovskaya, K. A.; Mikheeva, E. P.; Zhidomirov, G. M. *J. Mol. Catal., A., Chem.* **2002**, *178*, 191. Kachurovskaya, K. A.; Zhidomirov, G. M.; Minot, C. *Surf. Rev. Lett.* **2002**, *9*, 1425.
(15) Calatayud, M.; Mguig, B.; Minot, C. *Surf. Sci.* **2003**, *596*, 297.
(16) Khaliullin, R. Z.; Bell, A. T. *J. Phys. Chem. B* **2002**, *106*, 7832.

(17) Sayle, D. C.; Catlow, C. R. A.; Perrin, M. A.; Nortier, P. *J. Phys. Chem.* **1996**, *100*, 8940.

(18) Note that two definitions of the crystallographic axes of V_2O_5 are present in the literature. Here we choose the definition where the V_2O_5 layers are stacked along the *c*-direction, i.e., the basal plane is the (001) one. In the alternative definition the stacking direction is defined as the *b*-axis, so that the basal plane is the (010) one.

(19) Vittadini, A.; Selloni, A.; Rotzinger, F. P.; Grätzel, M. *Phys. Rev. Lett.* **1998**, *81*, 2954.

(20) Lazzeri, M.; Vittadini, A.; Selloni, A. *Phys. Rev. B* **2001**, *63*, 155409. Lazzeri, M.; Vittadini, A.; Selloni, A. *Phys. Rev. B* **2002**, *65*, 119901.

(21) Morishige, K.; Kanno, F.; Ogawara, S.; Sasaki, S. *J. Phys. Chem.* **1985**, *89*, 4404.

(22) Hadjiivanov, K. I.; Klissurski, D. G. *Chem. Soc. Rev.* **1996**, *25*, 61.

(23) Herman, G. S.; Sievers, M. R.; Gao, Y. *Phys. Rev. Lett.* **2000**, *84*, 3354. Hengerer, R.; Bolliger, B.; Erbudak, M.; Grätzel, M. *Surf. Sci.* **2000**, *460*, 162. Liang, Y.; Gan, S.; Chambers, S. A.; Altman, E. I. *Phys. Rev. B* **2001**, *63*, 235402.

(24) Lazzeri, M.; Selloni, A. *Phys. Rev. Lett.* **2001**, *87*, 266105.

(25) Vittadini, A.; Selloni, A.; Rotzinger, F. P.; Grätzel, M. *J. Phys. Chem. B***2000**, *104*, 1300. Vittadini, A.; Selloni, A. *J. Chem. Phys.* **2002**, *117*, 353.

(26) Car, R.; Parrinello, M. *Phys. Rev. Lett.* **1985**, *55*, 2741. Laasonen, K.; Pasquarello, A.; Car, R.; Lee, C.; Vanderbilt, D. *Phys. Rev. B* **1993**, *47*, 10142.

(27) Tassone, F.; Mauri, F.; Car, R. *Phys. Rev. B* **1994**, *50*, 10561.

(28) Perdew, J. P.; Burke, K.; Ernzerhof, M. *Phys. Rev. Lett.* **1996**, *77*, 3865.

(29) Vanderbilt, D. *Phys. Rev. B* **1990**, *41*, 7892.

(30) Baroni, S.; De Gironcoli; S. Giannozzi, P.; Dal Corso, A. *Program PWSCF 1.2.0*; http://www.pwscf.org.

(31) Taylor, D. *Trans. J. Brit. Ceram. Soc.* **1984**, *83*, 32.

(32) Kresse, G.; Surnev, S.; Ramsey, M. G.; Netzer, F. P. *Surf. Sci.* **2001**, *492*, 329.

(33) Vyboishchikov, S. F.; Sauer, J. *J. Phys. Chem. A* **2001**, *105*, 8588.

(34) Finnie, K. S.; Cassidy, D. J.; Bartlett, J. R.; Woolfrey, J. L. *Langmuir* **2001**, *17*, 816.

(35) Tilocca, A.; Selloni, A. *J. Chem. Phys.* **2003**, *119*, 7445.

(36) Hebenstreit, W.; Ruzycki, N.; Herman, G. S.; Gao, Y.; Diebold, U. *Phys. Rev. B* **2000**, *62*, R16334.

(37) Keller, D. E.; Weckhuysen, B. M. *Catal. Today* **2003**, *2811*, 1.

(38) Livage, J. Catal. Today **1998**, *41*, 3.

(39) Coulson, J. M.; Richardson, J. F. *Chemical Engineering*, 3rd ed.; Pergamon: Oxford, 1977; p 400.

(40) Model **M1** was built on the ordered hydroxylized surface, but we found that the energy of the analogous species on the scrambled surface is practically the same.

(41) Izumi, Y.; Kiyotaki, F.; Yoshitake, H.; Aika, K.; Sugihara, T.; Tatsumi, T.; Tanizawa, Y.; Shido, T.; Iwasawa, Y. *Chem. Commun.* **2002**, 2402.

(42) Laaksonen, L. *J. Mol. Graphics* **1992**, *10*, 33. Bergman, D. L.; Laaksonen, L.; Laaksonen, A. *J. Mol. Graphics Modelling* **1997**, *15*, 301. http://www.csc.fi/gopenmol/.